

Two-Dimensional Metallo-supramolecular Polymerization: Toward Size-Controlled Multi-strand Polymers

Jinne Adisojoso,[†] Yang Li,[†] Jun Liu,[‡] Pei Nian Liu,^{*,‡} and Nian Lin^{*,†}

[†]Department of Physics, The Hong Kong University of Science and Technology, Clear Water Bay, Hong Kong, China

[‡]Shanghai Key Laboratory of Functional Materials Chemistry and Institute of Fine Chemicals, East China University of Science and Technology, Meilong Road 130, Shanghai, China

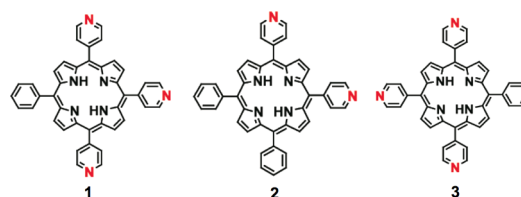
S Supporting Information

ABSTRACT: Multi-strand metallo-supramolecular polymers are self-assembled by pyridyl-functionalized porphyrin derivatives on a Au(111) surface through pyridyl–Cu–pyridyl coordination. Single-molecule-resolved characterization by scanning tunneling microscopy reveals a novel chain-growth polymerization mechanism for multi-strand supramolecular polymers. Furthermore, by varying the growth temperature and adding specific molecular modulators, both the length and the width of the polymers can be controlled.

Self-assembly of polymeric chains by reversible association of bifunctional or multifunctional monomers through specific non-covalent interactions (e.g., hydrogen bonding, metal–ligand coordination, p–p interaction, etc.) is a topic of intensive study.¹ Compared to covalent polymerization of organic monomers, the reversibility of supramolecular binding favors a high level of control toward thermodynamically equilibrated structures.² In particular, the reversibility of non-covalent bonds allows self-healing and error correction in supramolecular polymerization processes, which results in a high degree of structural perfection.³ The size of the supramolecular polymers, however, is difficult to control since the supramolecular polymerization is subject to subtle variation of external parameters, e.g., concentration of monomers, temperature, pH value, etc.⁴ On the other hand, since the supramolecular polymerization processes are highly dynamic, it remains a great challenge to acquire information on their size distribution which is crucial to understanding the polymerization mechanism.⁵ Taking advantage of the molecular resolution provided by scanning tunneling microscopy (STM) analysis,⁶ one can monitor the supramolecular polymer growth processes on surfaces in real time and precisely analyze the polymer size distribution, thus uncovering the underlying polymerization mechanism, which in turn can provide guidance on steering the polymerization processes and eventually realizing size control.

In this study, we chose pyridyl-functionalized porphyrin derivatives as the model system (Chart 1). The coordination self-assembly of the pure compounds with Cu on a Au(111) surface was described earlier.⁷ Herein, we report on an investigation of polymerization of multi-strand metallo-supramolecular chains self-assembled from mixtures of the compounds. By analyzing the length distribution of the polymers grown at different temperatures, we have identified a new polymerization mechanism. Furthermore, we demonstrate a strategy for

Chart 1. Molecular Structures of Three Porphyrin Derivatives: 5,10,15-Tri(4-pyridyl)-20-phenylporphyrin (1), 5,10-Di(4-pyridyl)-15,20-diphenylporphyrin (2), and 5,10,15,20-Tetra(4-pyridyl)porphyrin (3)



controlling the length as well as the width of the multi-strand metallo-supramolecular polymer chains using molecular modulators and substrate template effects.^{4c,5a}

In the presence of Cu, **1** forms a double-strand metallo-supramolecular polymeric chain structure in a ladder shape, aided by two-fold coordination of pyridyl–Cu–pyridyl on a Au(111) surface. A high-resolution STM image and the corresponding molecular model of the double-strand ladder are shown in Figure 1a,b. The molecular building blocks exhibit a high level of recognition, and double-strand ladders are found exclusively (cf.

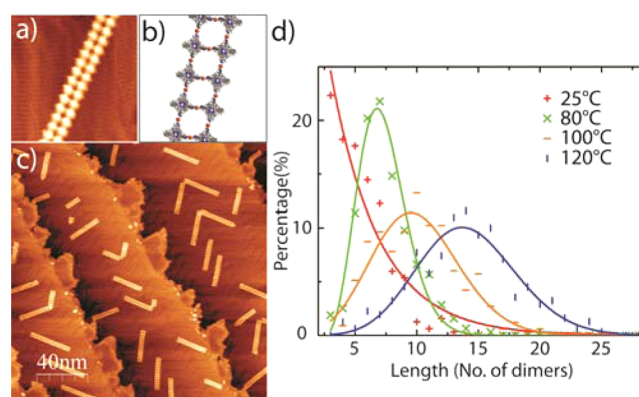


Figure 1. (a) High-resolution STM image ($20 \times 20 \text{ nm}^2$) of the double-strand ladder structure formed by **1** and Cu. (b) Corresponding molecular model of the double-strand ladder structure. (c) STM image of the sample after annealing at $120 \text{ }^\circ\text{C}$. (d) Length distributions of the sample after annealing at 25 (red), 80 (green), 100 (orange), and $120 \text{ }^\circ\text{C}$ (blue) with Flory–Schulz and Poisson fits.

Received: August 27, 2012

Published: October 17, 2012

Figure 1c). While intermolecular binding dictates the growth of the polymers, substrate–molecule interactions affect the orientation of the polymers with respect to the substrate crystalline directions.^{7b} This system offers an opportunity to understand the polymerization mechanism of double-strand polymers.⁸ According to STM data, the double-strand ladder chains exclusively end with a dimer; in other words, ladders ending with a single-strand tail have never been observed. This implies that the two strands grow collectively; i.e., growth of the double-strand ladder chains must propagate along the chain direction rather than adding monomers to an existing single strand. Such a process can be expected because collective growth offers one more bond and affords the more stable and rigid structure. Hence, it is valid to view the growth of the double-strand ladder chains as polymer growth.

To uncover the polymerization mechanism, we analyzed the length distribution of the double-strand ladders after annealing at different temperatures. Since the length of the double-strand ladders is directly accessible from the STM data, statistical analysis of many large-scale STM images provides an accurate account of the length distribution of the double-strand ladders (details on the analysis method can be found in SI). Figure 1d displays the length distribution at four different annealing temperatures, in which the percentage is calculated according to the number of double-strand ladders of different lengths with respect to the total number of double-strand ladders. At room temperature, the average length remains rather short, and the distribution shows a monotonous decay with increasing length. Upon increasing the annealing temperature, longer double-strand ladders become accessible. As shown in a typical STM image of the structures observed after annealing to 120 °C (Figure 1c), double-strand ladders of length up to 30 dimeric units can be observed (STM images of the sample at room temperature and annealed to 80 and 100 °C can be found in Figure S1). More interestingly, the length distribution transforms into a Poisson type. Furthermore, as shown in Figure 1d, the peak of the Poisson distribution is broadened and shifts to larger values with increasing temperature.

It has been reported that, in the solution phase, supramolecular polymerization is a step-growth (isodesmic supramolecular polymerization) process due to the equal reactivity of the supramolecular building blocks.^{5a} Flory predicted that step-growth polymerization results in a monotonous decay length distribution.⁹ An alternative mechanism—chain-growth—assumes that growth occurs through successive addition of monomers at the ends of the polymers. The latter growth mode results in a Poisson-type length distribution.⁹ In this study, **1** provides equal reactivity for coordination at its two ends; thus, at the first sight, the polymerization should be a step-growth process and the polymer length distribution should exhibit a monotonous decay character. However, the observed polymer length distribution is Poisson after annealing, which implies that the polymerization follows a chain-growth polymerization. This rather anomalous phenomenon suggests that the polymerization of the double-strand metallo-supramolecular chains on the surface follows a new mechanism: Unlike freely moving species in the solution phase, in the surface-supported metallo-supramolecular polymerization processes, the mobility of surface-adsorbed species is greatly reduced due to a surface diffusion barrier. The diffusion barrier is typically on the order of 0.5 eV for porphyrin monomers.^{7a} For n -meric ($n \geq 3$) clusters, the diffusion barrier becomes larger, and, consequently, the mobility of these clusters is significantly reduced; for example,

trimers or larger clusters are almost unmovable, as revealed by sequential STM scans at the experimental conditions. On the other hand, the coordination bond is weakened on the surface (0.2 eV for pyridyl–Cu coordination).^{7a} The competition of the diffusion energy barrier and the binding energy results in that the formed double-strand ladders do not move on the surface as an entity to bind with another ladder, but rather undergo dissociation into monomers. These free monomers, which are mobile on the surface, can readily attach to the ends of the existing ladders. Effectively, the growth of the polymers only happens through the addition of dimers at the ends of the existing ladders, i.e., following the chain-like growth mode. Hence, a subtle balance between the surface diffusion barrier and the binding energy results in the chain-growth polymerization mechanism, which expresses the Poisson distribution of the length distribution. Note that the monotonous decay length distribution observed for the sample prepared at 25 °C is due to kinetic hindrance, since the monomer mobility is not sufficient at this temperature, leading to the presence of a large amount of monomers. At higher annealing temperatures, the monomer diffusion barrier is overcome, and the system exhibits the thermodynamically favored Poisson distribution.

To achieve additional control of the chain length, we mixed **1** and **2** with Cu. Since **2** can saturate the end sites of the double-strand ladders, as illustrated in Figure 2b (molecules of **2** are colored in green), molecules of **2** can act as chain stoppers in polymer synthesis.^{10,5a} In order to avoid kinetically trapped structures, annealing at a temperature of 100 °C was applied for all mixtures in our experiments. Although STM cannot distinguish **1** from **2**, the effect of **2** is apparent: Figure 2a shows that the double-strand ladders become much shorter upon addition of **2**. The trimeric clusters are attributed to an excess of **2** molecules that do not participate in the formation of supramolecular chains.^{7b} The length reduction can be seen quantitatively in Figure 2c, which shows the length distribution of the double-strand ladders assembled at three different mixing ratios. The length distribution at a mixing ratio of 1:1 (cf. the green curve) exhibits a Poisson distribution with a narrower peak

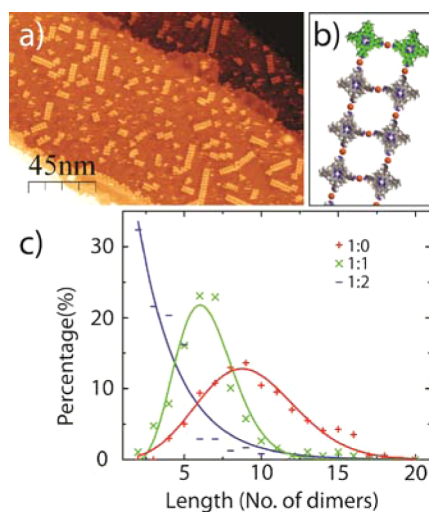


Figure 2. (a) STM image of a sample with **1** and **2** mixed in a ratio of 1:2 after annealing at 100 °C. (b) Model of a ladder end with **2** acting as a molecular stopper (in green). (c) Length distribution of the double-strand ladders formed at different mixing ratios (values shown indicate mixing ratio of **1** and **2**) with Flory–Schulz and Poisson fits.

appearing at a shorter length, indicating that the presence of **2** decreases the overall chain length compared with the chains formed out of pure **1** (cf. red curve). At a mixing ratio of 1:2 (cf. the blue curve in Figure 2c), the length distribution changes from the Poisson distribution to a monotonous decay. This observation is consistent with previous reports that the molecular stoppers can effectively reduce polymer length in solution-based polymerization.¹⁰ Note, however, the polymerization mechanism on surface is rather different from the one dictating the solution-based polymerization processes in 3D. Schmid et al. simulated a hypothesized chain-growth polymerization of dipotic monomers mixed with monotomic stoppers^{5a} and obtained chain length distributions at three mixing ratios that exhibit the exact same characteristics as the results shown in Figure 2c. The authors reported that experimentally, however, polymerization in the solution phase exhibited not the chain-growth but step-growth characteristics.^{5a} Our results demonstrate that supra-molecular polymerization at the surface obeys the chain-growth mechanism. As discussed before, this new mechanism exemplifies the templating role of surface. Note that, at a ratio of 1:2, the ideal structure is a ladder consisting of three dimeric units—a pair of molecules **1** sandwiched between two pairs of molecules **2**. However, the data show a broad distribution, indicating that precise control of the chain length is inaccessible, presumably due to entropic effects.

We have demonstrated that the length of the double-strand ladders can be controlled by varying the annealing temperature or adding molecular modulators, so the next question is, Can the width of the ladders be controlled to form multi-strand chains? We chose molecule **3** to modulate the width of the metallo-supramolecular polymer chains and again applied an annealing temperature of 100 °C to overcome kinetic trapping. Upon gradually increasing the amount of **3** in the mixture, ladders with three rows, i.e., triple-strand polymers, appeared besides the double-strand ones. These triple-strand ladders consist of two rows of **1**, bridged by a row of **3**, as illustrated in Figure 3a (molecules of **3** are colored in pink). Figure 3b summarizes the statistical analysis of the width distribution of the ladders at four different ratios of **1** and **3**. Surprisingly, a 2:1 ratio results in >96%

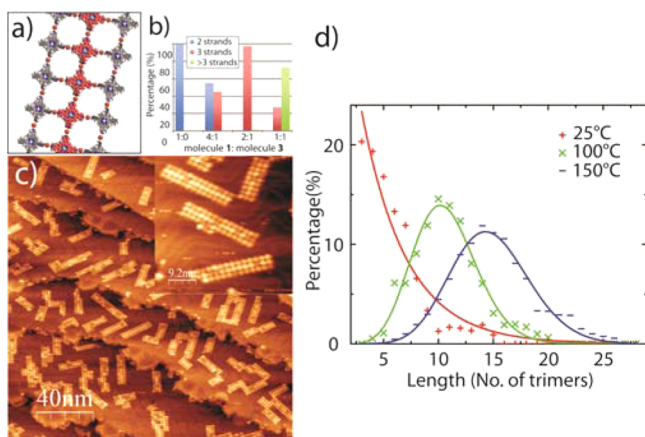


Figure 3. (a) Molecular model of the triple-strand ladder structure formed by **1** (gray) and **3** (pink). (b) Width distribution of the ladders at different ratios of **1** and **3**. (c) STM image of a 2:1 mixture of **1** and **3**, showing unique formation of the triple-strand ladders; inset, a high-resolution ($40 \times 40 \text{ nm}^2$) image of the triple-strand ladders. (d) Length distribution of the triple-strand ladders grown at 25 (red), 100 (green), and 150 °C (blue) with Flory–Schulz and Poisson fits.

formation of the triple-strand ladders. As shown in the STM image in Figure 3c, the majority of the ladders are triple-strand ladders. Even though the triple-strand ladders follow perfectly the 2:1 stoichiometry, a monodispersed width distribution is unexpected, considering that the entropic effect favors a broader width distribution; i.e., ladders of other widths (four-strand, five-strand, etc.) should appear. We found that a 2:1 ratio of **1** and **3** is crucial for the monodispersed triple-strand ladders and deviation from this ratio results in ladders of broader width distribution. For instance, adding more **3** leads to the formation of ladders of different widths and eventually to 2D patches (see Figure S2). As shown in Figure 3b, a 1:1 mixture of **1** and **3** does not form predominantly four-strand ladders that satisfy the stoichiometry.

The highly selective formation of triple-strand ladders implies that this structure is favored thermodynamically. In other words, the entropic effect is overcome by an enthalpy gain. Since the intermolecular interaction is equivalent for ladders of different widths, we attribute the enthalpy gain to molecule-to-surface interactions. It is well-known that molecules experience different molecule-to-surface interactions when adsorbed at different sites of the substrate atomic lattice.^{6b,11} As can be seen from the STM data, the long axis of the ladders mainly falls in three orientations on the surface, which signifies that the Au(111) substrate indeed modulates the growth of the ladders due to the uneven molecule-to-surface interaction. Presumably, in the triple-strand ladder structures, molecules are adsorbed in a specific adsorption configuration that gives rise to a larger molecule-to-surface binding energy, so the enthalpy gain is sufficient to overcome the entropic effect. This process resembles the template supra-molecular polymerization.^{4c} In contrast, in the four-strand or wider ladders, some molecules are adsorbed at less-favored sites, so the molecule-to-surface binding energy is not sufficient to beat entropy. This rather unique behavior demonstrates that a subtle variation of external parameters may decisively change the outcome of the supra-molecular polymerization processes. Nevertheless, a thorough understanding requires comprehensive theoretical investigations and is the subject of future research. We also studied the length distribution of the triple-strand ladders. A sample with a 2:1 ratio of **1** and **3** was subsequently annealed from 25 to 100 and 150 °C, respectively. Figure 3d shows that the ladder length is increased while the width is kept constant at three rows. The length distribution changes again from a monotonous decay to a Poisson distribution, indicating that the chain-growth polymerization mechanism is a general rule for the multi-strand supra-molecular polymers self-assembled on surfaces.

Finally, we attempted to control both dimensions, length and width, of the metallo-supramolecular polymers through mixing **1**, **2**, and **3** with Cu. Again, to overcome kinetically trapped structures, the samples were annealed at 100 °C. We found that as long as the ratio of **1** and **3** was kept at 2:1, the triple-strand ladders were formed predominantly. Figure 4a is a STM image showing the ladders self-assembled out of a mixture of **1**, **2**, and **3** in a ratio of 2:2:1. One can see that, in comparison to Figure 3c, the triple-strand ladders are relatively shorter. The lengths shown in Figure 4d (cf. the blue curve) exhibit a Poisson distribution with its peak at a shorter length compared with the fit for the ladders formed without **2** (cf. the red curve). As the amount of **2** is increased further, the Poisson distribution remains while the peak shifts to smaller values. In an ideal situation, a mixture of **1**, **2**, and **3** in a ratio of 4:4:1 may generate, as illustrated in Figure 4c, 3×3 squares consisting of four molecules of **2** at the four corners, four molecules of **1** at the four sides, and one molecule of

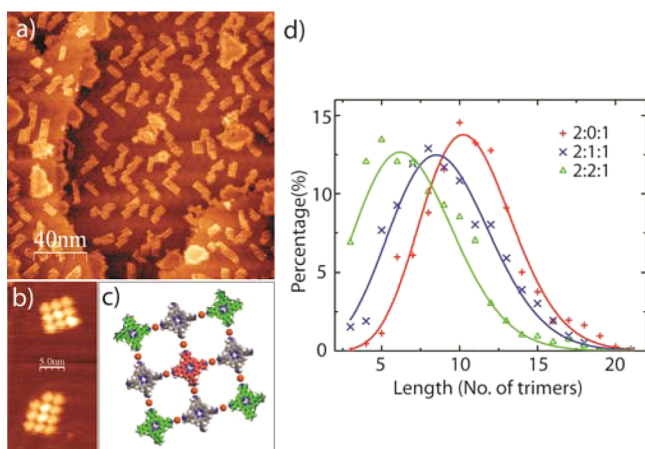


Figure 4. (a) STM image of a mixture of **1**, **2**, and **3** (ratio 2:2:1) showing the appearance of shorter triple-strand ladders. (b,c) High-resolution image of the 3×3 squares and corresponding molecular model (**1**, gray; **2**, green; and **3**, pink). (d) Length distribution of the triple-strand ladders (ratio 1:3 is set to 2:1) formed at different mixing ratios (values shown indicate mixing ratio of **1**, **2**, and **3**) with Poisson fits.

3 at the center. Drain et al. reported that, in the solution phase, such 3×3 square structures have been successfully synthesized at specific stoichiometries.¹² However, predominant formation of such 3×3 square structures was not realized with this mixing ratio in our experiments. Only in a few cases were such structures identified, as shown in Figure 4b. So far, we have not achieved precise control of both dimensions of the polymeric chains. There are several possible reasons: (1) the coordination bond is weakened substantially on the surface, so the entropy contribution becomes significant; (2) effective dissociation of the intermediate structures; (3) reduced freedom of molecular motion, hindering the error correction in the self-assembly; and (4) less-favored adsorption configuration of the 3×3 square structures on the surface.

In conclusion, Cu-coordinated multi-strand metallo-supramolecular polymers formed on a Au(111) surface were investigated using STM. Interestingly, for the first time, we find that the supramolecular polymerization of multi-strand polymers on a surface obeys the chain growth mechanism, which is different from the step-growth mechanism of the supramolecular polymerization in solution. We attribute this novel phenomenon to the collective growth of the strands and the subtle balance of the surface diffusion barrier and the intermolecular binding energy. Furthermore, we demonstrate that double-strand and triple-strand ladder structures could be formed monodispersedly, depending on the stoichiometry of the monomer compounds. Through interplay of growth temperature and the presence of molecular modulators, two-dimensional control over the polymer size, that is, length as well width, can be achieved. Our results provide molecular-level insight into the assembly process and mechanism of two-dimensional metallo-supramolecular polymerization.

■ ASSOCIATED CONTENT

Supporting Information

Synthesis, experimental procedure, data analysis, and supporting figures. This material is available free of charge via the Internet at <http://pubs.acs.org>,

■ AUTHOR INFORMATION

Corresponding Author

phnlin@ust.hk; liupn@ecust.edu.cn

Notes

The authors declare no competing financial interest.

■ ACKNOWLEDGMENTS

This work was supported financially by Hong Kong Research Council (Grant No. 603611), the National Natural Science Foundation of China (Project Nos. 21172069 and 21190033), and the Fundamental Research Funds for the Central Universities.

■ REFERENCES

- (1) (a) Lehn, J.-M. *Prog. Polym. Sci.* **2005**, *30*, 814. (b) Brunsveld, L.; Folmer, B. J. B.; Meijer, E. W.; Sijbesma, R. P. *Chem. Rev.* **2001**, *101*, 4071. (c) Moore, J. S. *Colloid Interface Sci.* **1999**, *4*, 108. (d) Capito, R. M.; Azevedo, H. S.; Velichko, Y. S.; Mata, A.; Stupp, S. I. *Science* **2008**, *319*, 1812.
- (2) (a) Zeng, F. W.; Zimmerman, S. C.; Kolotuchin, S. V.; Reichert, D. E. C.; Ma, Y. G. *Tetrahedron* **2002**, *58*, 825. (b) Sijbesma, R. P.; Beijer, F. H.; Brunsveld, L.; Folmer, B. J. B.; Hirschberg, J.; Lange, R. F. M.; Lowe, J. K. L.; Meijer, E. W. *Science* **1997**, *278*, 1601.
- (3) (a) Atwood, J. L.; Davies, J. E. D.; MacNicol, D. D.; Vögtle, F.; Lehn, J.-M., Eds. *Comprehensive Supramolecular Chemistry*; Pergamon: New York, 1996. (b) Lehn, J.-M. *Supramolecular Chemistry: Concepts and Perspective*; Wiley-VCH: Weinheim, 1995.
- (4) (a) De Greef, T. F. A.; Smulders, M. M. J.; Wolffs, M.; Schenning, A. P. H. J.; Sijbesma, R. P.; Meijer, E. W. *Chem. Rev.* **2009**, *109*, 5687. (b) Aida, T.; Meijer, E. W.; Stupp, S. I. *Science* **2012**, *335*, 813. (c) Janssen, P. G. A.; Jabbari-Farouji, S.; Surin, M.; Villa, X.; Gielen, J. C.; de Greef, T. F. A.; Vos, M. R. J.; Bomans, P. H. H.; Sommerdijk, N. A. J. M.; Christianen, P. C. M.; Leclère, P.; Lazzaroni, R.; van der Schoot, P.; Meijer, E. W.; Schenning, A. P. H. J. *J. Am. Chem. Soc.* **2008**, *131*, 1222.
- (5) (a) Schmid, S. A.; Abbel, R.; Schenning, A. P. H.; Meijer, E. W.; Sijbesma, R. P.; Herz, L. M. *J. Am. Chem. Soc.* **2009**, *131*, 17696. (b) Korevaar, P. A.; George, S. J.; Markvoort, A. J.; Smulders, M. M. J.; Hilbers, P. A. J.; Schenning, A. P. H. J.; De Greef, T. F. A.; Meijer, E. W. *Nature* **2012**, *481*, 492.
- (6) (a) De Feyter, S.; De Schryver, F. C. *J. Phys. Chem. B* **2005**, *109*, 4290. (b) Barth, J. V. *Annu. Rev. Phys. Chem.* **2007**, *58*, 375.
- (7) (a) Li, Y.; Lin, N. *Phys. Rev. B* **2011**, *84*, 125418. (b) Li, Y.; Adisoejoso, J.; Liu, J.; Liu, P. N.; Lin, N. Submitted. (c) Li, Y.; Xiao, J.; Shubina, T.; Chen, M.; Shi, Z.; Schmid, M.; Steinrueck, H.-P.; Gottfried, M.; Lin, N. *J. Am. Chem. Soc.* **2012**, *134*, 6401.
- (8) (a) Piguat, C.; Bernardinelli, G.; Hopfgartner, G. *Chem. Rev.* **1997**, *97*, 2005. (b) Chen, X. M.; Liu, G. F. *Chem.—Eur. J.* **2002**, *8*, 4811. (c) Mohr, F.; Jennings, M. C.; Puddphatt, R. J. *Angew. Chem.* **2004**, *116*, 987. (d) Ikeda, M.; Tanaka, Y.; Hasegawa, T.; Furusho, Y.; Yashima, E. *J. Am. Chem. Soc.* **2006**, *128*, 6806. (e) Ito, H.; Furusho, Y.; Yashima, E. *J. Am. Chem. Soc.* **2008**, *130*, 14008.
- (9) Flory, P. J. *Principles of Polymer Chemistry*; Cornell University Press: Ithaca, NY, 1953.
- (10) (a) Lortie, F.; Boileau, S.; Bouteiller, L.; Chassenieux, C.; Lauprêtre, F. *Macromolecules* **2005**, *38*, 5283. (b) Knoben, W.; Besseling, N. A. M.; Cohen Stuart, M. A. *Macromolecules* **2006**, *39*, 2643.
- (11) Lin, N.; Stepanow, S.; Ruben, M.; Barth, J. V. *Top. Curr. Chem.* **2009**, *287*, 1.
- (12) (a) Drain, C. M.; Batteas, J. D.; Flynn, G. W.; Milic, T.; Chi, N.; Yablon, D. G.; Sommers, H. *Proc. Natl. Acad. Sci. U.S.A.* **2002**, *6498*. (b) Milic, T. N.; Chi, N.; Yablon, D. G.; Flynn, G. W.; Batteas, J. D.; Drain, C. M. *Angew. Chem., Int. Ed.* **2002**, *41*, 2117.